Investigations of Complex Modes in a Generalized Bilateral Finline with Mounting Grooves and Finite Conductor Thickness

WEYL-KUO WANG, STUDENT MEMBER, IEEE, CHING-KUANG C. TZUANG, MEMBER, IEEE, JIING-SHYUE CHANG, AND TE-HUI WANG, MEMBER, IEEE

Abstract—A generalized bilateral finline with mounting grooves and finite conductor thickness is analyzed by a full-wave mode-matching method. The final nonstandard eigenvalue equation is derived from the unknown coefficients in the slot regions to reduce the size of the matrix equation. The convergence studies of the mode-matching method are first performed for the fundamental mode of a symmetric bilateral finline. Both the propagation constant and the characteristic impedance based on the power–voltage definition are analyzed and compared to the existing data. Excellent agreement between various data is obtained and the effects of metallization thickness and mounting grooves are discussed. The accurate results for the fundamental mode obtained by the mode-matching method with considerations of both relative and absolute convergences apply equally well to the analyses of the complex modes of the finline. The field matching plots at the slot–dielectric (air) interface of the finline also confirm that the converged solutions for the complex modes have superior field matchings over the nonconverged ones. The dispersion characteristics of the fundamental, higher order, evanescent, and complex modes are presented for an asymmetric bilateral finline. The effects of mounting grooves and metallization thickness on the complex mode propagation constants are investigated and discussed.

I. INTRODUCTION

SINCE THE introduction of the finline in 1972 [1], it has become an important class of transmission lines in millimeter-wave integrated circuits. To accurately characterize the electrical behavior of the various types of discontinuities which are frequently encountered in almost all the practical finline integrated circuits, many rigorous analytical techniques have been developed, e.g. the spectral-domain analysis by Zhang and Itoh [2], the transverse resonance technique by Sorrentino and Itoh [3], and the generalized scattering matrix (GSM) technique by a number of authors [4]–[6]. The authors in [2]–[6] dealt with the ideal finlines with infinitely thin metallizations or without mounting grooves. The influences of metallization thickness and mounting grooves can be pronounced at higher millimeter-wave frequencies [7]. The only analytical method reported to solve the generalized finline structure shown in Fig. 1 that takes into consideration both metallization thickness and substrate mounting grooves is the generalized transverse resonance method [8]–[10]. This technique is the modified mode-matching method combined with a transverse resonance relation. Regardless of the dimension of each region, the technique genuinely matches the boundary conditions associated with the dielectric, slot, and thick metal strip regions by an equal number of eigenfunction expansion terms for each region. It was mentioned briefly that the asymptotic behavior of the normalized propagation constants [10, fig. 2] is sufficient for 18 eigenfunction terms to be used for subsequent calculations in the paper. No further detailed investiga-

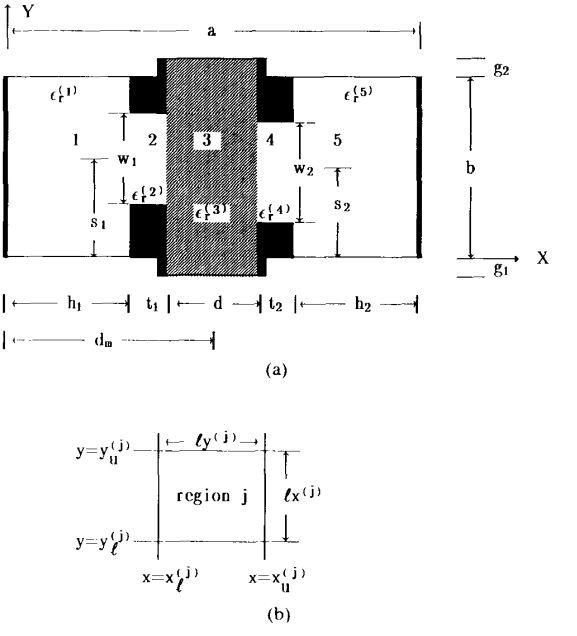

Fig. 1. Generalized finline with mounting grooves and finite metallization thickness. (a) Generalized finline configuration. (b) Notation for the corner coordinates and dimensions of a specific region j.

Manuscript received March 31, 1989; revised July 10, 1989. This work was supported in part by the National Science Council, Taiwan, R.O.C., under Grant NSC 78-0404-E009-16.

The authors are with the Institute of Communication Engineering, National Chiao Tung University, Hsinchu, Taiwan, R.O.C.

IEEE Log Number 8930814.

0018-9480/89/1200-1891$01.00 ©1989 IEEE

tions of the convergence properties of the propagation constants and characteristic impedance of the finline have been reported using the generalized transverse resonance method.

In this paper, the generalized finline configuration is analyzed by the conventional mode-matching method. The formulation varies the numbers of eigenfunction expansion terms from one region to another, when necessary. It makes it possible to investigate the relative and absolute convergence properties of the electromagnetic field solutions analyzed by the mode-matching method [11]. Many test cases are performed for both relative and absolute convergence studies and the optimal choice of ratios corresponding to the numbers of expansion terms in different regions is determined in a systematic way. By adopting the optimal choice of ratios, best field matchings along the interfaces between any two adjacent regions of the finline can be achieved. The optimal choice of ratios results in fast convergence for both the propagation constant and the characteristic impedance. If the optimal choice of ratios is violated, very poor field matchings will be obtained, and both the propagation constant and the characteristic impedance exhibit either slow or unpredictable convergence behavior. In certain cases they converge to wrong values. The effect of the relative convergence on the value of the characteristic impedance is found to be relatively significant compared to that on the propagation constant. Once the relative convergence study is completed, the absolute convergence study is initiated to obtain the minimal number of total expansion terms to save computer CPU time.

In addition, the existence of the complex modes in the generalized finlines has not been reported yet. Many reports have shown that neglecting the existing complex modes will cause substantial errors in waveguide step discontinuity problems [4], [12], [13]. As a direct result of the convergence studies, the solutions of the complex modes of the generalized finline can be sufficiently accurate for later analyses of the finline discontinuity problems. The effects of the metallization thickness and the finline mounting grooves on the guiding properties are fully investigated for the fundamental and the complex modes. For the fundamental mode, the theoretical values of propagation constant and characteristic impedance are checked against the existing data in [10] and [14]. Close results are obtained, and the differences are discussed [15]. Excellent agreement is obtained between the present paper and the results in [15], which analyzed the effect of the finite metallization thickness on the propagation constant and the characteristic impedance of a bilateral finline. Since the accuracy of the present approach is established, the effects of metallization thickness and mounting grooves on the complex modes are reported with confidence.

Finally, the fundamental, higher order, evanescent, and complex modes for a specific asymmetric bilateral finline are presented and the electric and magnetic field patterns of one of the complex modes plotted. This information serves as a prerequisite for finline discontinuity problems analyzed by the generalized scattering matrix technique.

II. Method of Analysis: Mode-Matching Method

A. Formulation

The generalized finline shown in Fig. 1, with each region arbitrarily extending in both the x and the y direction, is analyzed. Assuming the factor $e^{j\omega t-\gamma z}$, where $\gamma=\alpha+j\beta$, the full-wave hybrid TE-to-z and TM-to-z fields in each region i $(i=1,2,3,4,5)$ are derived from the Hertzian potentials ϕ and Ψ:

$$\vec{E}^{(i)}=\nabla\times\nabla\times\vec{e}_z\phi^{(i)}-j\omega\mu\nabla\times\vec{e}_z\Psi^{(i)}$$
$$\vec{H}^{(i)}=\nabla\times\nabla\times\vec{e}_z\Psi^{(i)}+j\omega\epsilon\nabla\times\vec{e}_z\phi^{(i)} \tag{1}$$

where $\vec{e}_z$ is the unit vector in the z direction.

The potentials $\phi^{(i)}$ and $\Psi^{(i)}$ are in terms of eigenfunction expansions satisfying the required boundary conditions in the y direction. They are summarized as follows.

Region 1:

$$\phi^{(1)}=\sum_{n=1}^{N_1}A_n fs_n^{(1)}(y)\sin\left(kx_n^{(1)}x\right)$$
$$\Psi^{(1)}=\sum_{n=0}^{N_1}B_n fc_n^{(1)}(y)\cos\left(kx_n^{(1)}x\right). \tag{2a}$$

Region j, $j=2,3,4$:

$$\phi^{(j)}=\sum_{n=1}^{N_j}fs_n^{(j)}(y)\left\{Fe_n^{(j)}\sin\left[kx_n^{(j)}\left(x-x_l^{(j)}\right)\right]+Ge_n^{(j)}\cos\left[kx_n^{(j)}\left(x-x_l^{(j)}\right)\right]\right\}$$
$$\Psi^{(j)}=\sum_{n=0}^{N_j}fc_n^{(j)}(y)\left\{Fh_n^{(j)}\sin\left[kx_n^{(j)}\left(x-x_l^{(j)}\right)\right]+Gh_n^{(j)}\cos\left[kx_n^{(j)}\left(x-x_l^{(j)}\right)\right]\right\}. \tag{2b}$$

Region 5:

$$\phi^{(5)}=\sum_{n=1}^{N_5}C_n fs_n^{(5)}(y)\sin\left[kx_n^{(5)}(a-x)\right]$$
$$\Psi^{(5)}=\sum_{n=0}^{N_5}D_n fc_n^{(5)}(y)\cos\left[kx_n^{(5)}(a-x)\right]. \tag{2c}$$

Here $fs_n^{(j)}(y)$ and $fc_n^{(j)}(y)$ are the y-directional eigenfunctions, i.e.,

$$fs_n^{(j)}(y)=\sin\left[n\pi\left(\frac{y-y_l^{(j)}}{ly^{(j)}}\right)\right]$$
$$fc_n^{(j)}(y)=\cos\left[n\pi\left(\frac{y-y_l^{(j)}}{ly^{(j)}}\right)\right]\Big/\sqrt{1+\delta_{n0}}. \tag{3}$$

In addition,

$$kx_n^{(j)}=\left[\epsilon_r^{(j)}k_0^2-\left(\frac{n\pi}{ly^{(j)}}\right)^2+\gamma^2\right]^{1/2}$$
$$k_0^2=\omega^2\mu_0\epsilon_0$$

δ_{mn} = Kronecker delta, and N_j is the number of eigenfunctions expansion terms in region j.

The boundary conditions need to be satisfied at the interfaces along $x = h_1$, $(h_1 + t_1)$, $(h_1 + t_1 + d)$, and $(h_1 + t_1 + d + t_2)$, respectively. A particular example of them can be expressed as

$$E_{y,z}^{(3)} = \begin{cases} E_{y,z}^{(2)} & y_l^{(2)} < y < y_u^{(2)} \\ 0 & y_l^{(3)} < y < y_l^{(2)}, \quad y_u^{(2)} < y < y_u^{(3)} \end{cases}$$

$$H_{y,z}^{(3)} = H_{y,z}^{(2)}, \qquad y_l^{(2)} < y < y_u^{(2)} \tag{4}$$

at $x = h_1 + t_1$.

Equations (2a)–(2c) indicate that 16 sets of unknown coefficients exist. The boundary conditions as typically shown in (4) contribute to 16 equations. It is possible to set up the nonstandard eigenvalue matrix equation after the coefficient elimination process. To save CPU time, the homogeneous matrix equation, i.e. (5), has the unknown coefficients associated with the slot regions:

$$[\boldsymbol{G}(\gamma)][\boldsymbol{x}] = \boldsymbol{0} \tag{5}$$

where

$$[\boldsymbol{G}(\gamma)] = ([\boldsymbol{V}(\gamma)] - [\boldsymbol{Q}(\gamma)])[\boldsymbol{D}(\gamma)]$$

$$[\boldsymbol{x}] = [\boldsymbol{Fh}^{(2)}\boldsymbol{Ge}^{(2)}\boldsymbol{Gh}^{(2)}\boldsymbol{Fe}^{(2)}\boldsymbol{Fh}^{(4)}\boldsymbol{Ge}^{(4)}\boldsymbol{Gh}^{(4)}\boldsymbol{Fe}^{(4)}]^T.$$

Each of the matrices $[\boldsymbol{G}]$, $[\boldsymbol{V}]$, $[\boldsymbol{Q}]$, and $[\boldsymbol{D}]$ has the size $4(N_2 + N_4 + 1)$ by $4(N_2 + N_4 + 1)$. The matrices $[\boldsymbol{Q}]$ and $[\boldsymbol{D}]$ contain diagonal submatrices only. The roots of the equation $\det([\boldsymbol{G}(\gamma)]) = 0$ give rise to the solutions for the propagation constants. Once the propagation constant is known, the coefficient vector $[\boldsymbol{x}]$ is solved within a constant multiplicative factor.

B. Characteristic Impedance

Applying the power–voltage definition, the characteristic impedance of the dominant mode of the finline is obtained by the expression

$$Z_0 = \frac{|V_s|^2}{2P_s} \tag{6}$$

where V_s is the voltage across the slot and P_s is the transported power associated with the slot, namely

$$V_s = \int_{y_l^{\text{slot}}}^{y_u^{\text{slot}}} E_y^{\text{slot}}(x_0, y)\, dy, \qquad x_0 \in (h_1, h_1 + t_1) \quad \text{or} \quad x_0 \in (h_1 + t_1 + d,\ h_1 + t_1 + d + t_2)$$

$$P_s = \begin{cases} \dfrac{1}{2}\,\text{Re} \displaystyle\sum_{i=1}^{5} \int\int_{S_i} \left(E_x^{(i)} H_y^{*(i)} - E_y^{(i)} H_x^{*(i)}\right) dx\,dy, & \text{for unilateral finlines} \\ \dfrac{1}{4}\,\text{Re} \displaystyle\sum_{i=1}^{5} \int\int_{S_i} \left(E_x^{(i)} H_y^{*(i)} - E_y^{(i)} H_x^{*(i)}\right) dx\,dy, & \text{for symmetric bilateral finlines.} \end{cases} \tag{7}$$

For all the cases presented in this paper, V_s varies less than 0.3 percent for x_0 in the interval $(h_1,\ h_1 + t_1)$ or $(h_1 + t_1 + d,\ h_1 + t_1 + d + t_2)$.

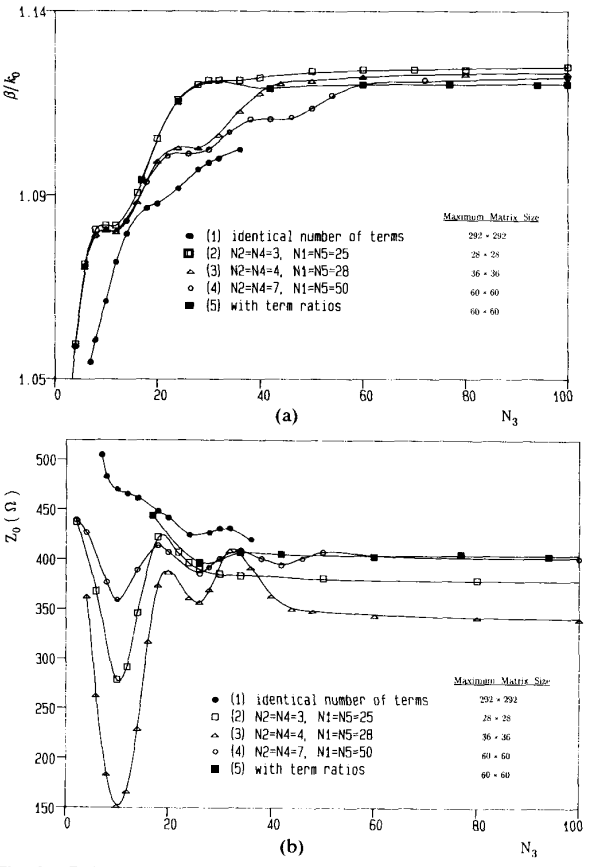

Fig. 2. Relative and absolute convergence studies for propagation constant and characteristic impedance of the fundamental mode of a symmetric bilateral finline with mounting grooves and finite conductor thickness at 50 GHz. $a = 2b = 7.112$ mm, $d = 125$ μm, $t_1 = t_2 = 5$ μm, $w_1 = w_2 = 0.5$ mm, $g_1 = g_2 = 0.35$ mm, $\epsilon_r^{(3)} = 3.75$, $\epsilon_r^{(1)} = \epsilon_r^{(2)} = \epsilon_r^{(4)} = \epsilon_r^{(5)} = 1$. (a) β/k_0 versus N_3. (b) Z_0 versus N_3.

Line (1): identical number of expansion terms ($N_1 = N_2 = N_3 = N_4 = N_5$).
Line (2): $N_2 = N_4 = 3$, $N_1 = N_5 = 25$.
Line (3): $N_2 = N_4 = 4$, $N_1 = N_5 = 28$.
Line (4): $N_2 = N_4 = 7$, $N_1 = N_5 = 50$.
Line (5): ratio of $N_j (j = 1,2,3,4,5)$ to N_3 is kept at the corresponding aspect ratio, i.e., $N_2 = N_4 \cong N_3(\frac{w_1}{b + g_1 + g_2})$ and $N_1 = N_5 \cong N_3(\frac{b}{b + g_1 + g_2})$.

III. Results

A. Convergence Studies for the Fundamental Mode

Fig. 2(a) and (b), which uses N_3 (the number of eigenfunction expansion terms in region 3 of Fig. 1) as the abscissa, depicts the convergence behavior of the propaga-

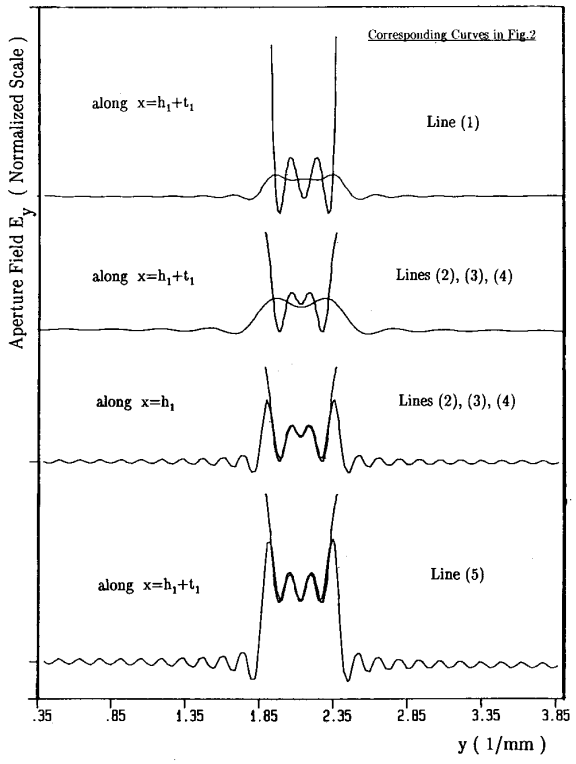

Fig. 3. Relative convergence studies of the aperture field E_y illustrating field matchings for four typical cases in Fig. 2. From top to bottom the plots correspond to:

E_y evaluated at $x = h_1 + t_1$, $N_1 = N_2 = N_3 = N_4 = N_5 = 36$;
E_y evaluated at $x = h_1 + t_1$, $N_2 = N_4 = 7$, $N_1 = N_5 = 50$, $N_3 = 24$;
E_y evaluated at $x = h_1$, $N_2 = N_4 = 7$, $N_1 = N_5 = 50$, $N_3 = 24$;
E_y evaluated at $x = h_1 + t_1$, $N_1 = N_5 = 50$, $N_2 = N_4 = 7$, $N_3 = 60$.

tion constant and the corresponding characteristic impedance of the fundamental mode of a symmetric bilateral finline with a 5 μm metallization thickness and a 0.35 mm groove depth, respectively. This is the same structure as previously analyzed by Bornemann and Arndt [10] using the generalized transverse resonance method (or the modified mode-matching method). Besides N_3, various combinations of expansion terms for other regions are chosen as the test conditions, designated as line (1) to line (5). Assuming all the eigenfunction expansion terms to be equal in number, the convergence behavior is represented by line (1) with solid circle symbols. Keeping the ratios of $N_1(N_5)$ to $N_2(N_4)$ equal to the aspect ratio b/w_1 and varying the ratios of N_3 to N_2 (and N_4), lines (2), (3), and (4) correspond to the test condition whereby the conformity of the ratio of eigenfunction [16] is satisfied at $x = h_1$ and $x = (a - h_2)$ and violated at $x = h_1 + t_1$ and $x = h_1 + t_1 + d$. With both the ratios of $N_1(N_5)$ to $N_2(N_4)$ and N_3 to N_2 (and N_4) kept the same as the aspect ratios b/w_1 and $(b + g_1 + g_2)/w_1$, respectively, the conformity of the ratio of eigenfunction expansions is satisfied at all slot interfaces. This corresponds to line (5).

The maximum matrix dimension for each line is also shown in Fig. 2. Line (1) depicts poor convergence even if the matrix is 292 by 292 in size. Lines (2), (3), and (4)

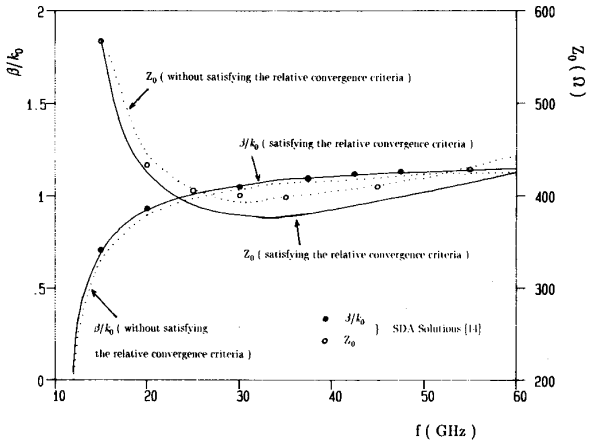

Fig. 4. Normalized propagation constant β/k_0 and characteristic impedance Z_0 of the fundamental mode as a function of frequency. Structural parameters: same as in Fig. 2.

····· (dotted lines) β/k_0 and Z_0 with $N_1 = N_2 = N_3 = N_4 = N_5 = 36$.

——— (solid lines) converged solutions of β/k_0 and Z_0 with $N_1 : N_2 : N_3 \cong b : w_1 : (w_1 + 2g_1)$.

● β/k_0 ○ Z_0 } SDA solutions after Schmidt and Itoh ($g_1 = g_2 = 0$, $t_1 = t_2 = 0$) [14].

converge to different asymptotic values. Line (5) illustrates the best convergence among all the test conditions since only five eigenfunction expansion terms (corresponding to N_3 equal to 42 in Fig. 2 and a matrix size of 44 by 44) in each slot region result in solutions that deviate by less than 0.2 percent from the converged ones.

The above-mentioned observation is attributed to the relative convergence phenomenon thoroughly discussed in [11] and [17]. The relative convergence phenomenon can be clearly observed from the E_y aperture field matching at $x = h_1 + t_1$, i.e., the interface between slot region 2 and groove region 3. Similar aperture field plots can be performed at other slot–dielectric (or air) interfaces. Fig. 3 plots the E_y aperture field matching at $x = h_1$ or $x = h_1 + t_1$. The results, from top to bottom of Fig. 3, are associated with the test conditions represented by lines (1), (2)–(4), and (5) of Fig. 2, respectively. It is clear that the resultant fields calculated by meeting the relative convergence requirement have the best field matching, as shown on the bottom two plots of Fig. 3.

Results illustrated by Figs. 2 and 3 confirm that the relative convergence criterion needs to be satisfied to obtain correct field solutions. Otherwise, the field solutions may not converge to correct values regardless of the size of the matrix $[G]$.

Fig. 4 plots the complete frequency dispersion characteristics of the fundamental mode with the same structural parameters as used in Figs. 2 and 3. Here three types of curves are generated for the propagation characteristics, namely, the SDA solutions [14] in circle symbols, solid lines for the mode-matching method satisfying relative convergence criteria, and dotted lines without satisfying the relative convergence criteria. Since the groove depth is one fifth of the half-waveguide height, it has a negligible

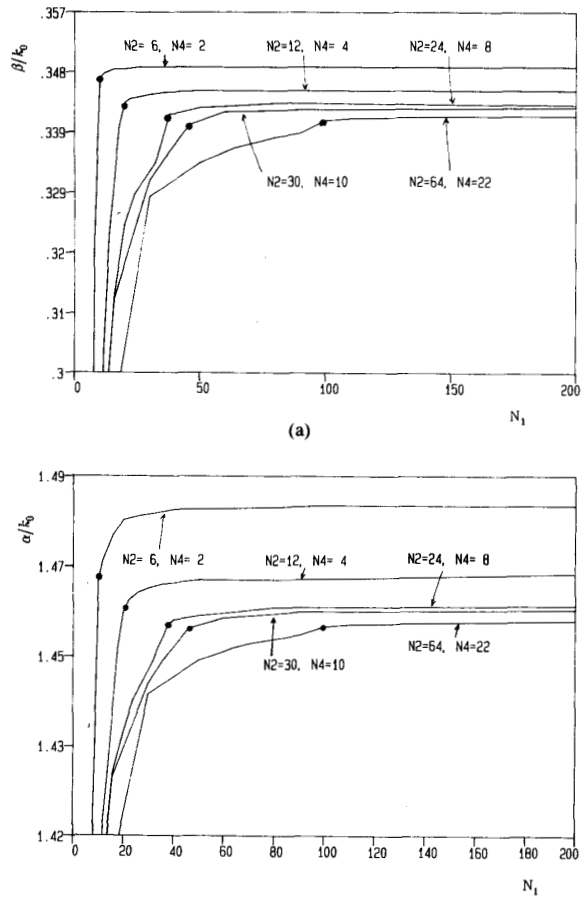

Fig. 5. Relative and absolute convergence studies of the normalized propagation constant of one of the complex modes versus the value of N_1 under different controlling parameters. $N_2=6$, $N_4=2$; $N_2=12$, $N_4=4$; $N_2=24$, $N_4=8$; $N_2=30$, $N_4=10$; $N_2=64$, $N_4=22$. $N_2/N_4 \cong 3$, $N_1=N_3=N_5$. $a=2.032$ mm, $b=1.27$ mm, $s_1=s_2=b/2$, $d_m=0.85$ mm, $\epsilon_r^{(3)}=12$, $\epsilon_r^{(1)}=\epsilon_r^{(2)}=\epsilon_r^{(4)}=\epsilon_r^{(5)}=1$, $d=32\%b$, $t_1=t_2=1$ mil, $w_1=64\%b$, $w_2=22\%b$, $g_1=g_2=0$. (a) β/k_0 versus N_1. (b) α/k_0 versus N_1.

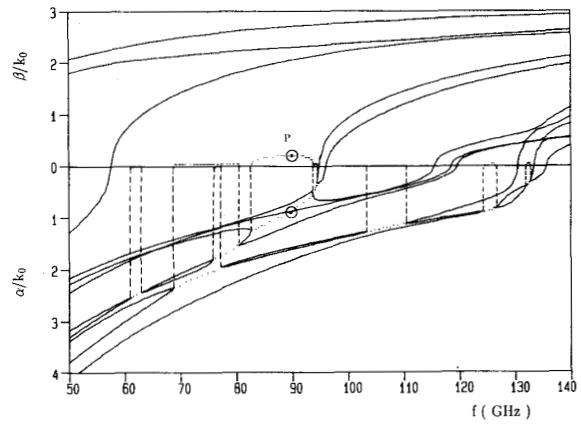

Fig. 6. Normalized propagation constant versus frequency for an asymmetric bilateral finline with mounting grooves and finite metallization thickness. $a=2.54$ mm, $b=1.27$ mm, $d=30\%b$, $t_1=t_2=0.7$ mil, $w_1=30\%b$, $w_2=45\%b$, $s_1=65\%b$, $s_2=57.5\%b$, $d_m=42.5\%a$, $g_1=g_2=2.5$ mils, $\epsilon_r^{(3)}=10$, $\epsilon_r^{(1)}=\epsilon_r^{(2)}=\epsilon_r^{(4)}=\epsilon_r^{(5)}=1$.

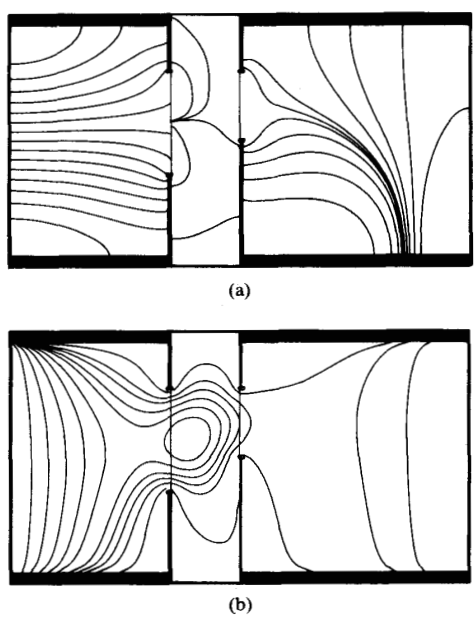

Fig. 7. Electric and magnetic field patterns of the complex mode at point P of Fig. 6. $f=90$ GHz, $\gamma/k_0=0.84775+j0.20412$, $\omega t=0°$, 60×34 points. (a) Electric field pattern. (b) Magnetic field pattern.

effect on the dispersion characteristics of the dominant mode [7]. The fact that the metallization thickness tends to lower the value of the characteristic impedance for the dominant mode of a bilateral or a unilateral finline has been reported in the literature [15]. Excellent agreement to the data reported in the literature [15, e.g. fig. 7] is obtained by the present approach. When comparing the results for the characteristic impedance, the solid line is indeed lower than that obtained by the SDA. The dotted line has the opposite effect, which indicates that the field solution is not accurate. Similar conclusion can be drawn for the propagation constant.

B. Relative and Absolute Convergence Studies for the Complex Modes

The procedure for the relative convergence studies performed in the previous section has been successfully extended to the complex modes. Similar results of the convergence studies were reported in [18]. Only the expanded final results are reported here, as shown in Fig. 5. The solid dotted symbols in Fig. 5(a) and (b) correspond to the condition whereby the relative convergence criteria are met at both slot regions. Thus very good convergence properties are achieved in this case. It is interesting to note that the complex modes require bigger matrix size or more eigenfunction expansion terms to have the converged propagation constants within 0.2 percent of their converged values. In one particular case of Fig. 5, $N_2=30$, $N_4=10$

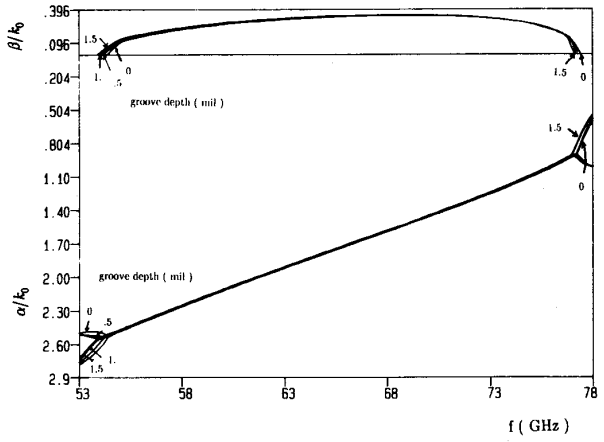

(a)

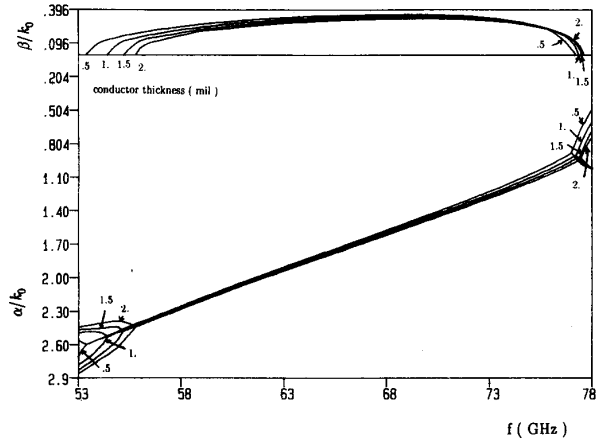

(b)

Fig. 8. Effects of metallization thickness and groove depth on the propagation constant of one of the complex modes. Structural parameters the same as in Fig. 5. (a) β/k_0 and α/k_0 versus groove depth g. (b) β/k_0 and α/k_0 versus conductor thickness t.

($N_1 = N_3 = N_5$), 0.2 percent accuracy is obtained. But the matrix size is 164 by 164, in contrast to that of 44 by 44 for the fundamental mode reported earlier.

C. Dispersion Characteristics of Fundamental, Higher Order, Evanescent, and Complex Modes in a Generalized Bilateral Finline with Mounting Grooves and Finite Metallization Thickness

The normalized propagation constants versus frequency for an asymmetric bilateral finline with mounting grooves and finite metallization thickness are presented in Fig. 6. Notice that the relative dielectric constant is 10, much lower than the value used in [19]. The complex modes exist in and outside the full W-band region (75–110 GHz). The third and fourth higher order modes have split into complex modes already.

The electric and magnetic field patterns [20] of a particular complex mode (corresponding to point P of Fig. 6) are plotted in Fig. 7(a) and (b), respectively. The field distributions of this specific complex mode exhibit strong interactions with the sidewalls, in contrast to the fundamental mode, which has most of its electromagnetic energy confined near the slot regions. As expected, across the air–dielectric interface, the normal component of the electric field is stronger in the air region while the magnetic field lines are continuous and may form closed loops.

The influences of the groove depth and of the metallization thickness of the finline on one of the complex modes are illustrated in Fig. 8(a) and (b), respectively. The effects of the metallization thicknesses are seen to be greater than those of various groove depths. The groove depth and the metallization thickness have opposite effects on the complex modes. The former tends to shift the complex mode region to the lower frequency and the latter to the higher frequency. Similar results are observed for the symmetric unilateral finlines.

IV. Conclusion

Extensive studies of the convergence properties of the propagation characteristics for the generalized finline configuration indicate that the relative convergence criterion previously applied to a single waveguide step discontinuity problem can still hold for the particular finline structure with dual slots. The relative convergence criterion helps to reduce the matrix size required to obtain accurate electromagnetic field solutions based on the mode-matching method. If the relative convergence criterion is violated, the propagation constant may still converge, but the aperture field matching will be poor. Depending on whether the modal solution belongs to the fundamental mode or the complex modes, the eigenfunction expansion terms (or the matrix size) may vary to reach the same accuracy. The latter requires more expansion terms.

The relative convergence criterion will be extended to a finline configuration with more than two slots. The accuracy of the finline step discontinuity problem formulated by the generalized scattering matrix (GSM) approach depends on correct modal field solutions. Since GSM formulism incorporates dominant, higher order, evanescent, and complex modes, any inaccurate modal solutions on both sides of the discontinuity will contribute to the accumulative errors associated with the GSM formulism. Thus it is believed that the present approach will substantially improve the accuracy of modeling the discontinuity characteristics for a finline with fairly complicated cross-sectional geometry.

Acknowledgment

The authors wish to thank Prof. D. Kajfez, Department of Electrical Engineering, University of Mississippi, for kindly providing the software [20] to plot the continuous field lines shown in Fig. 7.

References

[1] P. J. Meier, "Two new integrated-circuit media with special advantages at millimeter wavelengths," in *IEEE MTT-S Int. Microwave Symp. Dig.*, 1972, pp. 221–223.

[2] Q. Zhang and T. Itoh, "Spectral-domain analysis of scattering from *E*-plane circuit elements," *IEEE Trans. Microwave Theory Tech.*, vol. MTT-35, pp. 138–150, Feb. 1987.
[3] R. Sorrentino and T. Itoh, "Transverse resonance analysis of finline discontinuities," *IEEE Trans. Microwave Theory Tech.*, vol. MTT-32, pp. 1633–1638, Dec 1984.
[4] A. S. Omar and K. Schünemann, "The effect of complex modes at finline discontinuities," *IEEE Trans. Microwave Theory Tech.*, vol. MTT-34, pp. 1508–1514, Dec 1986.
[5] M. Helard, J. Citerne, O. Picon, and V. F. Hanna, "Theoretical and experimental investigation of finline discontinuities," *IEEE Trans. Microwave Theory Tech.*, vol. MTT-33, pp. 994–1003, Oct. 1985.
[6] R. R. Mansour and R. H. Macphie, "An improved transmission matrix formulation of cascaded discontinuities and its application to *E*-plane circuits," *IEEE Trans. Microwave Theory Tech.*, vol. MTT-34, pp. 1490–1498, Dec. 1986.
[7] R. Vahldieck and W. J. R. Hoefer, "The influence of metallization thickness and mounting grooves on the characteristics of finlines," in *IEEE MTT-S Int. Microwave Symp. Dig.*, 1985, pp. 143–144.
[8] R. Vahldieck, "Accurate hybrid-mode analysis of various finline configurations including multilayered dielectrics, finite metallization thickness and substrate holding grooves," *IEEE Trans. Microwave Theory Tech.*, vol. MTT-32, pp. 1454–1460, Nov. 1984.
[9] R. Vahldieck and J. Bornemann, "A modified mode-matching technique and its application to a class of quasi-planar transmission lines," *IEEE Trans. Microwave Theory Tech.*, vol. MTT-33, pp. 916–926, Oct. 1985.
[10] J. Bornemann and F. Arndt, "Calculating the characteristic impedance of finlines by transverse resonance method," *IEEE Trans. Microwave Theory Tech.*, vol. MTT-34, pp. 85–92, Jan. 1986.
[11] T. S. Chu and T. Itoh, "Comparative study of mode–matching formulations for microstrip discontinuity problems," *IEEE Trans. Microwave Theory Tech.*, vol. MTT-33, pp. 1018–1023, Oct. 1985.
[12] J. Strube and F. Arndt, "Rigorous hybrid-mode analysis of the transition from rectangular waveguide to shielded dielectric image guide," *IEEE Trans. Microwave Theory Tech.*, vol MTT-33, pp. 391–401, May 1985.
[13] K. A. Zaki, S. W. Chen, and C. Chen, "Modeling discontinuities in dielectric-loaded waveguides," *IEEE Trans. Microwave Theory Tech.*, vol. 36, pp. 1804–1810, Dec. 1988.
[14] L. P. Schmidt and T. Itoh, "Spectral domain analysis of dominant and higher order modes in finlines," *IEEE Trans. Microwave Theory Tech.*, vol. MTT-28, pp. 981–985, Sept. 1980.
[15] T. Kitazawa and R. Mittra, "Analysis of finline with finite metallization thickness," *IEEE Trans. Microwave Theory Tech.*, vol. MTT-32, pp. 1484–1487, Nov. 1984.
[16] F. J. K. Lange, "Analysis of shielded strip- and slot-lines on a ferrite substrate transversely magnetized in the plane of the substrate," *Arch. Elek. Übertragung.*, vol. 36, pp. 95–100, 1982.
[17] R. Mittra, T. Itoh, and T. S. Li, "Analytical and numerical studies of the relative convergence phenomenon arising in the solution of an integral equation by the moment method," *IEEE Trans. Microwave Theory Tech.*, vol. MTT-20, pp. 96–104, Feb. 1972.
[18] W-K. Wang, C-K. C. Tzuang, C-Y. Shih, and T-H. Wang, "Investigations of complex modes in a generalized bilateral finline with mounting grooves and finite conductor thickness," in *IEEE MTT-S Int. Microwave Symp. Dig.*, 1989, pp. 491–494.
[19] A. S. Omar and K. Schünemann, "Formulation of the singular integral equation technique for planar transmission lines," *IEEE Trans. Microwave Theory Tech.*, vol. MTT-33, pp. 1313–1322, Dec. 1985.
[20] D. Kajfez and J. A. Gerald, "Plotting of vector fields with a personal computer," *IEEE Trans. Microwave Theory Tech.*, vol. MTT-35, pp. 1069–1072, Nov. 1987.

✠

Weyl-Kuo Wang (S'88) was born in Taiwan, Republic of China, on October 29, 1963. He received the B.S. degree in communication engineering from the National Chiao Tung University, Hsinchu, Taiwan, in 1986. Since 1987, he has been working toward the Ph.D. degree at the same university. His current research interests include waveguide discontinuity problems and their applications to millimeter integrated circuits.

Ching-Kuang C. Tzuang (S'84–M'87) was born in Taiwan on May 10, 1955. He received the B.S. degree in electronic engineering from the National Chiao Tung University, Hsinchu, Taiwan, in 1977 and the M.S. degree from the University of California at Los Angeles in 1980.

From February 1981 to June 1984, he was employed at TRW, Redondo Beach, CA, working on analog and digital monolithic microwave integrated circuits. He received the Ph.D. degree in electrical engineering in 1986 from the University of Texas at Austin, where he worked on high-speed transient analyses of monolithic microwave integrated circuits. Since September 1986, he has been with the Institute of Communication Engineering, National Chiao Tung University, Hsinchu, Taiwan, R.O.C. He is currently conducting research on millimeter-wave and microwave integrated circuit technology.

✠

Jiing-Shyue Chang was born in Taiwan, Republic of China, on November 18, 1965. He received the B.S. degree in electrical engineering from the National Sun Yat-Sen University, Kaohsiung, Taiwan, in 1988. Since September 1988, he has been working toward the M.S. degree in communication engineering at the National Chiao Tung University, Hsinchu, Taiwan. His topics of interests include modal analyses of quasi-planar transmission lines and finline discontinuity problems.

✠

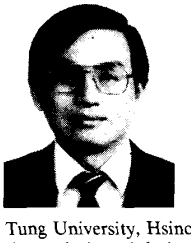

Te-Hui Wang (S'86–M'88) was born in Taichung, Taiwan, Republic of China, on May 16, 1954. He received the B.Sc. degree in physics from National Tsing Hua University, Taiwan, in 1977, the M.E. degree from the Tatung Institute of Technology, Taiwan, in 1981, and the Ph.D. degree from the University of Texas at Austin in 1988.

He is now with the Chung Shung Institute of Science and Technology, Lung Tan, Taiwan. He is also a part-time professor at National Chiao Tung University, Hsinchu, Taiwan. His current research interests include the analysis and design of microwave and millimeter-wave components.